Research Article | Vol. 27, No. 20 / 30 September 2019 / Optics Express 29055

Optics EXPRESS

Light-controlled skyrmions and torons as reconfigurable particles

HAYLEY R. O. SOHN,[1] CHANGDA D. LIU,[1] YUHAN WANG,[1] AND IVAN I. SMALYUKH[1,2,3,*]

1

[redacted]

Optics EXPRESS

regions of the sample changes, with the free energy associated with embedding individual solitons

Optics EXPRESS

a single integrated optical setup. Optical imaging was done using a BX51 Olympus upright microscope equipped with a charge-coupled device camera (purchased from Point Grey Research, Inc.), crossed polarizers above and below the sample, 4x, 10x, and 20x dry objectives (numerical apertures ranging from 0.3 to 0.9), and a red filter (Edmund Optics). Finely focused patterns of blue light were projected onto the samples using the LC micro-displays of an Epson EMP-730 LC Projector that were integrated with the BX51 microscope (Fig. 4b) using lenses and a dichroic mirror (DM 505LP) that reflects the blue patterning light but transmits the red imaging light from the microscope light source [41]. With this setup, the blue patterning light is in the 450-480 nm range and has an intensity on the order of 1 nW per square micron [41]. Because of the relatively long wavelength of the blue patterning light and the thin 10 μm cell thickness, absorbance within the LC sample doped with low concertation of additives is negligible and the illumination can be considered of constant intensity throughout the cell depth [38,43]. The experimental images and videos were analyzed using open source ImageJ/FIJI software (obtained from the National Institute of Health), through which positional data for each video frame was extracted using built-in particle tracking capabilities.

In order to obtain computer-simulated images of the director field configurations, we use a MATLAB-based numerical approach to minimize the Frank-Oseen free energy of the LC (Eqn. 1) [11,26,29]. Computer-simulated polarizing optical images are then based on these energy-minimizing structures with experimental material parameters, such as birefringence, Δn,

Fig. 3. Skyrmion dimensions with changing pitch. (a, b) Computer-simulated skyrmions in a chiral nematic LC shown at (a) d/p = 0.925 and (b) d/p = 1.25, where the vectorized **n(r)** is colored according to orientations on the $\mathbb{S}^2$ sphere (inset). (c) Simulated skyrmion diameter measured within the d/p stability range, where sample thickness is fixed at 10 μm and corresponding diameters from (a) and (b) are marked in red, inset with simulated polarizing optical microscopy images corresponding to parts (a) and (b). (d, e) Experimentally measured

Optics EXPRESS

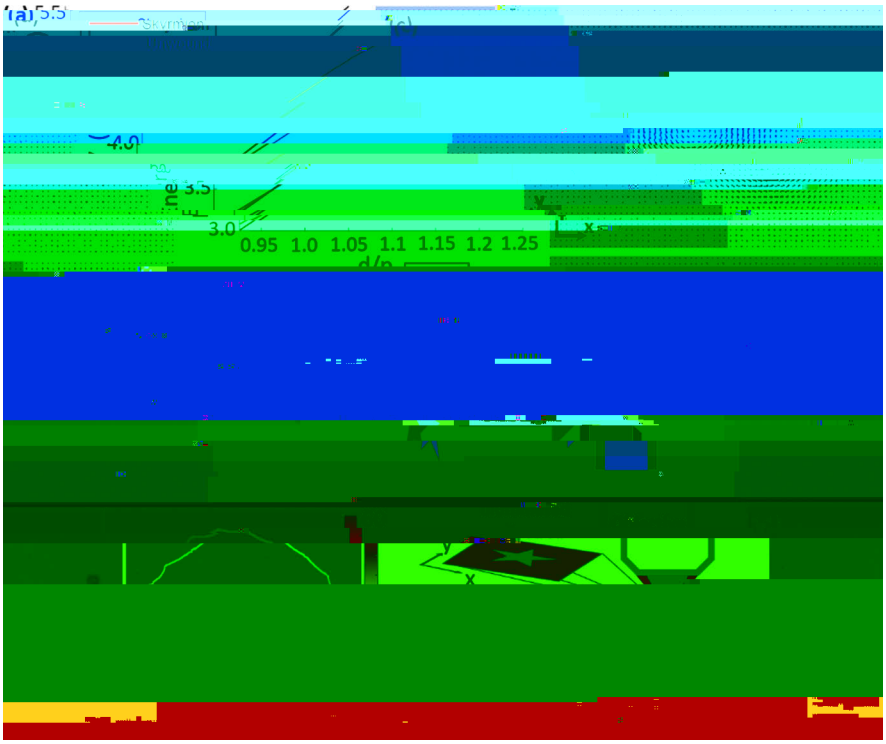

Fig. 4. Patterned light projection for controlled skyrmion motion. (a) Elastic free energy dependence of the twisted skyrmionic state (red) and the unwound or homeotropic state (black) on d/p. Energy was computed numerically on a 100 µm x 100 µm x 32 µm computational volume. (b) Experimental setup for blue-light patterning projection with red imaging light, polarizer (*P*), analyzer (*A*), dichroic mirror (*DM 505LP*), and charge-coupled device camera (*CCD*, PointGrey, FlyCap) labeled. 4x, 10x, and 20x Olympus dry objectives were used. (c) Computer-simulated demonstration of skyrmion propagation, where the blue region represents illumination and black rods represent **n(r)** orientation. (d) Experimental patterned-light-induced motion of a skyrmion in a spiral path, the trajectory of which is shown overlaid on the polarizing images and colored according to elapsed time in seconds (right-side inset). Crossed polarizer and analyzer orientations are marked with white double arrows.

and cell thickness, d, and generated using a Jones matrix method [29,44]. The material parameters used in all computer simulations correspond to independently characterized experimental values (Table 1), where n_{ext} and n_{ord} represent the extraordinary and ordinary refractive indices of the nematic host E7.

4. Results and discussion

By selectively patterning μm^2-to-cm^2 areas within the chiral nematic LC samples using blue-light illumination, we gain optical control over the free-energy landscape within the chiral nematic sample. Because our skyrmions are stabilized by the chirality of the material, selective manipulation of the cholesteric pitch in various regions throughout the sample can tune their dimensions and dynamics. Therefore, when allowed to move, skyrmions and torons always tend to escape into the darker regions of illumination patterns, but responses can be even more complex if such dynamics is somehow hindered or if changes of pitch occur faster than these topological solitons can move. By harnessing these facile optical response e□ects, we demonstrate a high

Optics EXPRESS

level of experimental control by probing individual skyrmions, large skyrmion lattices, and skyrmion bags, as detailed below.

Optics EXPRESS

Fig. 5. Skyrmion-toron structure evolution with changing pitch. (a, b) Numerically simulated vertical cross-sections of torons in a chiral nematic LC shown in the cross-sectional plane containing the far-field director at (a) d/p = 0.925 and (b) d/p = 1.25, where the vectorized **n(r)** is colored according to orientation on the $\mathbb{S}^2$ sphere (inset). (c, d) Computer-simulated demonstration of photo-induced skyrmion propagation shown in the cross-sectional plane containing the far-field director, where the blue region represents the part of sample under illumination and black rods represent **n(r)** orientation. Numerical simulations are based on material parameters of nematic host E7 and left-handed chiral additive QL-76 (see Methods), with d = 10 μm. A similar E7 – QL-76 mixture was used in experiment, details of which are reported in Table 1.

4.2. Control of symmetry and parameters of skyrmion lattices

We demonstrate optically reconfigurable control over arrays of solitons and study an assortment of materials-science inspired demonstrations by generating various periodic lattices with large skyrmion densities (Fig. 6–8). By using a checkerboard-like illumination pattern we reversibly rearrange a hexagonal/triangular lattice of solitons (Fig. 6a) to a square-periodic lattice (Fig. 6d) and back (Fig. 6f) over the course of about 10 minutes. This is done by translating the illumination pattern with the skyrmions closely following the dark regions of the pattern. The direction of the pattern translation determines the direction of skyrmion motions because these solitons tend to stay in the dark regions of the pattern to keep their free energy at minimum. While skyrmions embedded in a uniform homeotropic background are known to interact repulsively [45], which is consistent with the hexagonal lattice under the conditions of a large number density of skyrmions per unit area [25], our findings show that light can drive assembly of out-of-equilibrium crystalline lattices of solitons, like the square-periodic lattice. Considering that skyrmions exhibit Brownian motions and particle-like behavior, the light-controlled solitonic assemblies can potentially provide a platform to investigate structural phase transitions in condensed matter, e.g. between equilibrium and out-of-equilibrium 2D crystalline lattices.

Interestingly, various types of defects can be embedded into these lattices as well. When we start from defining a grain boundary between two hexagonal lattices of topological solitons (Fig. 7) and expose the upper and lower boundaries, the energetic gradient becomes such that the inner part of the grain boundary is more energetically favorable for the skyrmions. The illumination therefore pushes the solitons together into a healed lattice without a grain boundary, towards an equilibrium state (Fig. 7a). Time-coded colored trajectories show how the solitons move smoothly towards each other (Fig. 7b) and how the many-body interactions between them eventually realize the lattice that corresponds to an equilibrium organization at large number-density of skyrmion particles. We also demonstrate precise control of the energetic gradient and resulting solitonic motion that allows for creation and healing of a small crack in a close-packed hexagonal lattice

Optics EXPRESS

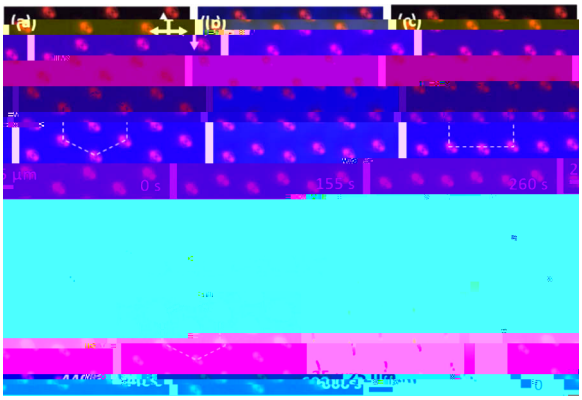

Fig. 6.

Optics EXPRESS

lattice due to repulsive interactions. However, when starting from crystallites that have been defined and optically oriented with a 20-degree o□set in each of their lattice vectors (Fig. 9c), the coarsening of packing defects takes a much longer time (Fig. 9b) because the merging of the nucleated crystallites initially leads to the creation of grain boundaries. The evolution to an energetically favorable hexagonal-packed crystallite requires more rearrangement of skyrmions to align the crystallographic vectors by annealing the grain boundaries. The misalignment of LC or crystalline domains during ordered phase nucleation at the first-order phase transition is known to often lead to defects, with one example being the Kibble-Zurek mechanism of forming defects by merging nematic drops with misaligned director orientations [48,49]. Interestingly, although they are realized in chiral nematic hosts without intrinsic positional ordering, these skyrmionic particle-like structures may reveal details of how grain boundary defects form and behave during 2D crystallization transitions, mediating formation of polycrystalline materials.

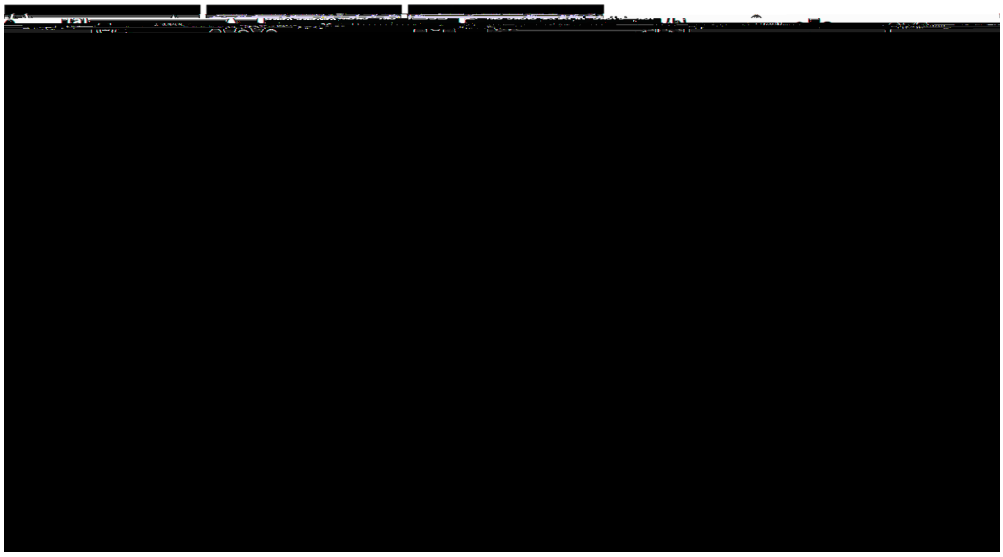

Fig. 9. Merging of skyrmion crystallites. (a) Polarizing optical microscopy images of three aligned skyrmion crystallites nucleating upon circular boundary illumination to form one large crystallite. (b) Schematics of aligned crystallites upon nucleation, with boundary skyrmions colored according to number of nearest neighbors (red = 5, black = 6). (c) Polarizing optical microscopy images of three misaligned skyrmion crystallites nucleating under similar illumination to form one large crystallite. (d) Schematics of misaligned crystallites upon nucleation, with boundary skyrmions colored according to number of nearest neighbors (blue = 4, red = 5, black = 6). Crossed polarizer orientation is marked with white double arrows and elapsed time is noted in the bottom right corner of images. The material is E7 doped with QL-76.

On the other hand, the interactions of elementary skyrmions in high energy and nuclear physics models allows for understanding the nature of subatomic particles with high baryon numbers [9,24]. While LC and magnetic 2D analogs of these skyrmions tend to mutually repel, it is possible to form high-degree condensed matter analogs of these high baryon number particles through formations of skyrmion bags and related structures [45]. This may again allow for using our soft matter system as a testbed for exploring and understanding complex topological phenomena. The skyrmion number of a skyrmion bag depends on the number of anti-skyrmions (N_A) embedded within it, where a bag described by $S(N_A)$ has a topological degree $N_A - 1$ [45]. Here, using an approach similar to that described previously [45], we generate large skyrmion

Optics EXPRESS

bags with skyrmion numbers close to 100 in our photo-sensitive cells as a means of studying their manipulation in the same way that we've characterized degree-one individual skyrmion photosensitivity. First, we probe the bag under full-area blue light illumination, similar to the experiments shown in Fig. 3. As the pitch increases across the entire sample area in the absence of an energy gradient, the skyrmions within the bag shrink in diameter, as expected, and the bag shrinks in size (Fig. 10a). Similar to an individual skyrmion's behavior under these conditions, the bag grows back to it equilibrium dimensions with elapsed time in the absence of blue-light illumination. Next, we induce an energetic gradient by means of illumination on the left side

Optics EXPRESS

healing and crack propagation, lattice compression, crystallite merging during nucleation, and transformations of skyrmion bags. Considering that these skyrmions are hosted in anisotropic LC materials, our findings may lead to photo-responsive photonic gratings and di□raction patterns, privacy windows (note that the intensity of light utilized to control skyrmions is comparable to that of ambient light), and even new touch-screen technologies. Although various types of optical control of skyrmionics structures in condensed matter have been demonstrated previously by using specially designed beams of light [19,26,32,50,51], our work enables such control when using unstructured light of intensity comparable to that of ambient light, which can expand the potential technological uses of skyrmions in LCs.

Funding

National Science Foundation (ACI-1532235, ACI-1532236, DGE-1144083, DMR-1810513).

Acknowledgments

We thank T. Bunning and T. White for providing the QL-76 chiral dopant used throughout this study. We also thank P. Ackerman, C. Bowman, J-S. B. Tai, T. White, R. Voinescu, and Y. Yuan for useful discussions. I.I.S. acknowledges hospitality of the Newton institute at Cambridge University during his stay, when part of the manuscript preparation was completed.

References

1. T. Dauxois and M. Peyrard, *Physics of solitons*. Cambridge University Press. (2006).
2. M. J. Ablowitz, *Nonlinear dispersive waves: asymptotic analysis and solitons* (Vol. 47). Cambridge University Press. (2011).
3. Y. S. Kivshar and G. Agrawal, *Optical solitons: from fibers to photonic crystals*. Academic press. (2003).
4. Z. Chen, M. Segev, and D. N. Christodoulides, "Optical spatial solitons: historical overview and recent advances," Rep. Prog. Phys. **75**(8), 086401 (2012).
5. G. Assanto and M. A. Karpierz, "Nematicons: self-localized beams in nematic liquid crystals," Liq. Cryst. **36**(10-11), 1161–1172 (2009).
6. Y. V. Izdebskaya, A. S. Desyatnikov, G. Assanto, and Y. S. Kivshar, "Deflection of nematicons through interaction with dielectric particles," J. Opt. Soc. Am. B **30**(6), 1432 (2013).
7. A. Alberucci, A. Piccardi, U. Bortolozzo, S. Residori, and G. Assanto, "Nematicon all-optical control in liquid crystal light valves," Opt. Lett. **35**(3), 390–392 (2010).
8. Y. V. IzdebskaExprtioBl(Y)105(.)-250(Desy)30(atnik)30(7(shar)42nd)-2502G. Assancu, G [-86(xprtioBl(Y)102S.)-250(Kiv)20(shar)42o,Wn20Nemat7

Optics EXPRESS

22. T. Van Mechelen and Z. Jacob, "Photonic Dirac monopoles and skyrmions: spin-1 quantization," Opt. Mater. Express **9**(1), 95–111 (2019).
23. L. Du, A. Yang, A. V. Zayats, and X. Yuan, "Deep-subwavelength features of photonic skyrmions in a confined electromagnetic field with orbital angular momentum," Nat. Phys. **15**(7), 650–654 (2019).
24. N. Manton and P. Sutcli□e, *Topological solitons*. Cambridge University Press. (2004).
25. P. J. Ackerman, J. van de Lagemaat, and I. I. Smalyukh, "Self-assembly and electrostriction of arrays and chains of hopfion particles in chiral liquid crystals," Nat. Commun. **6**(1), 6012 (2015).
26. I. I. Smalyukh, Y. Lansac, N. A. Clark, and R. P. Trivedi, "Three-dimensional structure and multistable optical switching of triple-twisted particle-like excitations in anisotropic fluids," Nat. Mater. **9**(2), 139–145 (2010).
27. P. J. Ackerman, Z. Qi, and I. I. Smalyukh, "Optical generation of crystalline, quasicrystalline, and arbitrary arrays of torons in confined cholesteric liquid crystals for patterning of optical vortices in laser beams," Phys. Rev. E **86**(2), 021703 (2012).
28. P. J. Ackerman, Z. Qi, Y. Lin, C. W. Twombly, M. J. Laviada, Y. Lansac, and I. I. Smalyukh, "Laser-directed hierarchical assembly of liquid crystal defects and control of optical phase singularities," Sci. Rep. **2**(1), 414 (2012).
29. P. J. Ackerman, T. Boyle, and I. I. Smalyukh, "Squirming motion of baby skyrmions in nematic fluids," Nat. Commun. **8**(1), 673 (2017).
30. H. R. O. Sohn, P. J. Ackerman, T. J. Boyle, G. H. Sheetah, B. Fornberg, and I. I. Smalyukh, "Dynamics of topological solitons, knotted streamlines, and transport of cargo in liquid crystals," Phys. Rev. E **97**(5), 052701 (2018).
31. H. R. O. Sohn, C. D. Liu, and I. I. Smalyukh, "Schools of skyrmions with electrically tunable elastic interactions,"*Nat. Commun.*(2019).
32. W. Yang, H. Yang, Y. Cao, and P. Yan, "Photonic orbital angular momentum transfer and magnetic skyrmion rotation," Opt. Express **26**(7), 8778–8790 (2018).
33. P. Milde, D. Köhler, J. Seidel, L. M. Eng, A. Bauer, A. Chacon, J. Kindervater, S. Mühlbauer, C. Pfeiderer, S. Buhrandt, C. Schütte, and A. Rosch, "Unwinding of a skyrmion lattice by magnetic monopoles," Science **340**(6136), 1076–1080 (2013).
34. T. J. White, R. L. Bricker, L. V. Natarajan, N. V. Tabiryan, L. Green, Q. Li, and T. J. Bunning, "Phototunable azobenzene cholesteric liquid crystals with 2000nm range," Adv. Funct. Mater. **19**(21), 3484–3488 (2009).
35. Y. Wang and Q. Li, "Light-driven chiral molecular switches or motors in liquid crystals," Adv. Mater. **24**(15), 1926–1945 (2012).
36. Y. C. Hsiao, K. C. Huang, and W. Lee, "Photo-switchable chiral liquid crystal with optical tristability enabled by a photoresponsive azo-chiral dopant," Opt. Express **25**(3), 2687–2693 (2017).
37. G. S. Chilaya, "Light-controlled change in the helical pitch and broadband tunable cholesteric liquid-crystal lasers," Crystallogr. Rep. **51**(S1), S108–S118 (2006).
38. Q. Li, L. Green, N. Venkataraman, I. Shiyanovskaya, A. Khan, A. Urbas, and J. W. Doane, "Reversible photoswitchable axially chiral dopants with high helical twisting power," J. Am. Chem. Soc. **129**(43), 12908–12909 (2007).
39. P. G. De Gennes and J. Prost, *The physics of liquid crystals* (Vol. 83). Oxford University Press. (1995).
40. J. S. Evans, P. J. Ackerman, D. J. Broer, J. van de Lagemaat, and I. I. Smalyukh, "Optical generation, templating, and polymerization of three-dimensional arrays of liquid-crystal defects decorated by plasmonic nanoparticles," Phys. Rev. E **87**(3), 032503 (2013).
41. Y. Yuan, G. N. Abuhaimed, Q. Liu, and I. I. Smalyukh, "Self-assembled nematic colloidal motors powered by light," Nat. Commun. **9**(1), 5040 (2018).
42. Y. Yuan, Q. Liu, B. Senyuk, and I. I. Smalyukh, "Elastic colloidal monopoles and out of equilibrium interactions in liquid crystals," Nature **570**, 214–218 (2019).
43. J. Ma, Y. Li, T. White, A. Urbas, and Q. Li, "Light-driven nanoscale chiral molecular switch: reversible dynamic full range color phototuning," Chem. Commun. **46**(20), 3463–3465 (2010).
44. P. Yeh and C. Gu, *Optics of liquid crystal displays* (Vol. 67). John Wiley & Sons. (2010).
45. D. Foster, C. Kind, P. J. Ackerman, J.-S. B. Tai, M. R. Dennis, and I. I. Smalyukh, "Two-dimensional skyrmion bags in liquid crystals and ferromagnets," Nat. Phys. **15**(7), 655–659 (2019).
46.